

Low ratio of sediment recycling at Northeast Japan Arc: Constraints from ^{10}Be isotopes and B-Ba-K-Be systematics

TAKASHI SANO,^{1*} TOSHIKI HASENAKA,² AKIKO SHIMAOKA,³ TAKAAKI FUKUOKA⁴ and HISAO NAGAI⁵

¹Department of Geology and Paleontology, National Museum of Nature and Science, 4-1-1 Amakubo, Tsukuba, Ibaraki 305-0005, Japan

²Faculty of Advanced Science and Technology, Kumamoto University, 2-39-1 Kurokami, Chuo-ku, Kumamoto-shi, Kumamoto 860-8555, Japan

³Earthquake Research Institute, The University of Tokyo, 1-1-1 Yayoi, Bunko-ku, Tokyo 113-0032, Japan

⁴Faculty of Geo-Environmental Sciences, Rissho University, 1700 Magechi, Kumagaya, Saitama 360-0914, Japan

⁵College of Humanities and Sciences, Nihon University, 3-25-40 Sakurajosui, Setagaya-ku, Tokyo 156-8550, Japan

(Received April 8, 2016; Accepted December 29, 2016)

The contribution of subducted sediments to the compositions of arc magmas is now widely accepted, but ratios of the sediment recycling have not been examined in detail. Here we compare the Be isotopes and B-Ba-K-Be systematics of descending sediments and erupted lavas from a cold subduction zone, the Northeast (NE) Japan Arc, to examine the sediment recycling. The descending sediments were recovered from Japan Trench, and erupted lavas were collected from three active volcanoes on the volcanic front of the NE Japan Arc. Since the subducting slab is cold, the pressure-temperature (P-T) path of its upper surface does not cross the sediment solidus, which means that the sediments would not be melted and release hydrous fluids to the overlying mantle wedge. In addition to the sediment-derived fluid, contributions of fluids from subducted altered oceanic crust (AOC) is proposed to satisfy the Be isotopes and B-Ba-K-Be systematics. Comparisons of NE Japan to other cold subduction zones show that ^{10}Be input from Japan Trench ($^{10}\text{Be} = 488 \times 10^6$ atoms/g; $^{10}\text{Be}/^9\text{Be} = 471 \times 10^{-11}$) is middle range, but ^{10}Be output from NE Japan volcanoes is lower ($^{10}\text{Be} < 0.8 \times 10^6$ atoms/g; $^{10}\text{Be}/^9\text{Be} < 3.1 \times 10^{-11}$) than the other arcs (Kurile and Tonga-Kermadec arcs). This fact suggests that the ratio of sediment recycling at the NE Japan Arc is distinctly lower than the other cold subduction zones. The low ratio of sediment recycling is probably due to the lower temperature of descending slab beneath the NE Japan Arc than the other arcs, because cold slab induces both low extraction rate of Be from descending slab and long travel time beneath the arcs. Also, significant scraping of sediments from descending slab is another candidate to explain the low extraction rate of ^{10}Be .

Keywords: arc magma, trench sediment, recycling, beryllium-10, Northeast Japan

INTRODUCTION

Subduction zones are the only major routes by which material extracted from the mantle can be returned to great depths within the Earth, contributing to mantle heterogeneity (e.g., Iwamori and Albarède, 2008; Kimura *et al.*, 2016). The dominant surface expression of subduction is the curved chains of active volcanoes that form island arcs; the magmatic flux in these volcanoes is an important component of new additions of mantle material to the crust. Therefore, an understanding of subduction processes and the origins of arc magma are among the main goals of the Earth sciences. Given that the involvement of subducted sediment and its underlying altered oceanic crust (AOC) and serpentinized peridotites in the genera-

tion of arc magmas has been confirmed by analyses of geochemical tracers (e.g., Ishikawa and Nakamura, 1994; Elliott *et al.*, 1997; Turner and Hawkesworth, 1997; Ryan and Chauvel, 2014; Savov *et al.*, 2007), it is important to examine ratios of the subducted materials to arc crust. Among the potential geochemical tracers, we employed four in this study. First, we chose Be isotope ($^{10}\text{Be}/^9\text{Be}$) because the most convincing evidence for the involvement of subducted sediment in arc magma is the discovery of quantities of ^{10}Be in arc lavas (e.g., Tera *et al.*, 1986; Morris *et al.*, 1990). Some of the subducted sediment recycled at subduction zones should allow at least part of the sedimentary load of ^{10}Be to survive (half life = 1.36 Myr; Nishiizumi *et al.*, 2007) and to re-emerge in arc lavas if recycled. The second tracer, the element B, is arguably the most powerful for evaluating the recycling of sediments, AOC and serpentinites (Morris *et al.*, 1990; Leeman *et al.*, 1994; Ryan *et al.*, 1995; Bebout, 2007), because it is strongly enriched in all three components.

*Corresponding author (e-mail: sano@kahaku.go.jp)

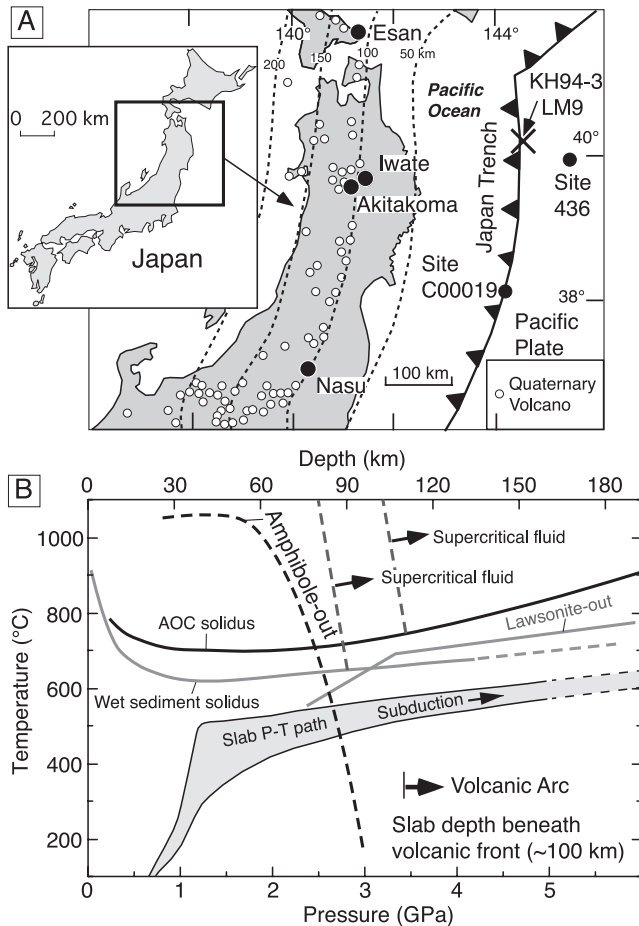


Fig. 1. (A) Map of the NE Japan Arc showing the location of Iwate, Akitakoma, Nasu, and Esan volcanoes, and the distribution of Quaternary volcanoes. Sample locations of sediments entering the Japan Trench at KH-94-3 LM9, DSDP Site 436, and IODP C00019 are also shown. The counters show the depth of the upper surface of the subducting slab (Hasegawa *et al.*, 1994). The inset shows the location of the main map. (B) P-T diagram showing the hydrous solidi of sediment (Nichols *et al.*, 1994) and AOC (Schmidt and Poli, 1998), the stability field of amphibole and lawsonite (Schmidt and Poli, 1998), and the thermal structure in the subduction zone of the NE Japan Arc (Iwamori, 2007). The nearly vertical dashed lines represent the critical curves of supercritical fluids for sediment (Kawamoto *et al.*, 2012) and AOC (Mibe *et al.*, 2011), respectively.

The third and fourth tracers, Ba and K, are widely used to detect contributions of the AOC and biogenic sediment in arc magmas (e.g., Elliott, 2003; Plank, 2014). Other mobile elements (e.g., Rb, Th) are also used as tracers but are less powerful than B, Ba and K.

The optimal situation for quantifying sediment subduction is where $^{10}\text{Be}/^9\text{Be}$ ratios in arc lavas correlate with other tracers that are also dominated by subduction contributions. A good correlation between $^{10}\text{Be}/^9\text{Be}$ and B/

Be points to the isotopic composition of the sediment component added to the mantle (Morris *et al.*, 1990; Morris and Ryan, 2004). We expand examination of the correlation by the use of Ba/Be and $\text{K}_2\text{O}/\text{Be}$ in this study.

The NE Japan Arc is possibly the best site worldwide for estimating the ratio of sediment recycling because its tectonic setting is well documented (e.g., Hasegawa *et al.*, 1994). This arc formed in response to westward subduction of old (129 Ma; Syracuse *et al.*, 2010) Pacific Plate beneath NE Japan (Fig. 1A). Since the subducting slab is old and cold, the P-T path of its upper surface does not cross the sediment or AOC solidi up to 5 GPa (160 km), which means that neither the sediment nor the AOC are melting in the upper surface of the slab (Fig. 1B). Instead, the AOC is partly dehydrated and releases fluid to the overriding mantle wedge at a depth of ~90 km, in response to the breakdown of amphibole (Fig. 1B). Since the P-T path of the slab at deep levels has not been determined in detail, the exact depth of the dehydration of hydrous minerals (lawsonite and phengite) in the sediment is unclear, but is probably >180 km (Fig. 1B). The fluids from serpentinized peridotites in subducted slab are likely to generate arc magmas because contribution of high B isotope ratios of the Mariana forearc serpentinites ($\delta^{11}\text{B} > +12\%$; Benton *et al.*, 2001) can explain higher ratios of Izu-Mariana basalts ($\delta^{11}\text{B} +3\%$ to $+8\%$; Ishikawa and Nakamura, 1994; Ishikawa and Tera, 1999) than sediments and AOC (generally $\delta^{11}\text{B} < +3\%$; Spivack *et al.*, 1987; Smith *et al.*, 1995).

In this paper we provide concentrations of geochemical tracers and other elements in 35 sediment samples from the Japan Trench (at KH94-3 LM9) and in 22 lavas from three volcanoes (Iwate, Akitakoma, Nasu) on the volcanic front of the NE Japan Arc (Fig. 1A). High precision data of ^{10}Be and $^{10}\text{Be}/^9\text{Be}$ in 11 lava samples were recently published by Shimaoka *et al.* (2016), but most geochemical data are original of this study (Supplementary Tables S1 and S2). Depth profiles of ^{10}Be , B/Be, Ba/Be and $\text{K}_2\text{O}/\text{Be}$ are used to estimate sediment input from Japan Trench, and the estimated input values are compared to data of other cold subduction zones (Kurile and Tonga-Kermadec arcs) that were previously reported (George *et al.*, 2005; Dreyer *et al.*, 2010). The sediment input data are compared with ^{10}Be , B/Be, Ba/Be and $\text{K}_2\text{O}/\text{Be}$ in lavas from the cold subduction zones, and then ratios of sediment recycling are examined. To evaluate crustal contamination beneath NE Japan Arc, geochemical data of 5 rocks from the upper crust are also reported.

SAMPLE AND ANALYTICAL METHODS

Samples

The sediments were collected using a 10 m piston core at the central part of the Japan Trench ($40^\circ 27.89' \text{N}$,

144°29.35' E; water depth 7451 m) during cruise KH-94-3 of the R/V *Hakuho-maru* (Fig. 1A). The samples are brown to brownish-black pelagic clays containing no visible carbonate (Sano *et al.*, 2001).

The samples from Iwate volcano are six Younger Iwate Lavas that include samples reported by Sano *et al.* (2001) and 11 Older Iwate Lavas (Nakagawa, 1987). The Older Iwate samples are six tholeiitic rocks from the Onimata Lava and five calc-alkaline rocks from the Onashiro Lava (Table S1). Eruption ages of the Younger Lavas are younger than 3000 BC and those of the Older Lavas are older than 3000 BC. All the Younger Iwate Lavas are tholeiitic. The Younger Iwate samples were collected from three lava flows, namely the Myoko, Yakushidake, and Yakehashiri lavas (Nakagawa, 1987). We also collected five basement rocks of the Iwate volcano to examine the effect of wall rock (i.e., crustal rocks) contamination by the Iwate magma. The crustal rocks sampled are three plutonic rocks and two tuffaceous rocks (Table S1). Volcanic rocks from the Nasu and Akitakoma volcanoes were collected from a Numahara Lava (<8000 BC) and a lava from Odake cone (<1000 BC), respectively. The Nasu and Akitakoma samples were previously used to analyze Sr isotope composition (Notsu, 1983). The phenocryst assemblages of the volcanic rocks and the mineral assemblages of the plutonic rocks are described in Table S1.

Analytical methods

Major and selected trace element (Rb, Ba, Sr, Zr, Y, Cr, Ni, V) contents were determined using a Rigaku RIX2100 X-ray fluorescence (XRF) spectrometer at Fuji Tokoha University, Japan, following the method of Sano (2002). Rock samples were broken in an iron mortar and sieved to millimeter-sized chips. Only fresh chips were handpicked and washed ultrasonically, twice in alcohol and twice in distilled water. The cleaned chips were dried for >12 hours in an oven at 110°C and then ground to powder in an agate mill. Glass beads were prepared from the powders for XRF analyses, using anhydrous lithium tetraborate ($\text{Li}_2\text{B}_4\text{O}_7$) as a flux. Each sample powder was mixed with the $\text{Li}_2\text{B}_4\text{O}_7$ flux in the proportion of 1 to 5 and then fused at 1100°C in a $\text{Pt}_{95}\text{Au}_5$ crucible to be shaped into a glass bead. Analytical precision data, as estimated from repeated analyses of a well-established reference standard (JB-1a), are given in Table S1, and additional precision data are given in Sano (2002). For selected samples of the sediments, weight loss on ignition (LOI) was determined (Table S2); about 1.0 g of powder was weighed on a Metler Toledo dual balance system and heated at 1025°C for 4 hours in an electric muffle furnace. Replicated analyses of the samples shows that uncertainty on the LOI is 0.03 wt%. We also analyzed Nb contents using a Rigaku RIX1000 XRF spectrometer at the National Museum of Nature and Science, Tokyo, Ja-

pan following the method of Sano *et al.* (2011). For the Nb analyses, about 4.0 g of powder was pressed into a pellet by a 15 ton force from a hydraulic press, and then analyzed.

B, Sm, and Gd contents were determined by prompt gamma neutron activation analysis (PGNA) at the thermal neutron beam guide of the JRR-3M reactor, Japan Atomic Energy Research Institute, Tokai-mura, Japan, following the methods of Sano *et al.* (1999, 2006). The sample powders (0.6–0.8 g) were cold-pressed into disks (12 mm in diameter and 2–3 mm thick) that were heat-sealed in 25- μm -thick fluorinated ethyleneprophylene resin film smaller than $14 \times 14 \text{ mm}^2$. A Compton suppression prompt gamma activation spectrum was accumulated for 6000–7200 s. Geological Survey of Japan standards JB-1 and JB-2 were used to calibrate the B, Sm, and Gd contents. Replicate analyses of JB-1 and JB-2 indicate overall precision and accuracy of ~3% for B and Gd, and 10% for Sm (Sano *et al.*, 1999, 2006).

A non-destructive instrumental neutron activation analysis (INAA) technique was used for analyses of Cs, Th, Hf, and rare earth elements (La, Ce, Nd, Sm, Eu, Tb, Yb, Lu, Sc). The sample powders (0.1–0.2 g) were activated for 6 hours in reactor TRIGA-II of the Institute for Atomic Energy, Rikkyo University, Japan. Simultaneously, JB-1 and JR-2 (standard rocks from the Geological Survey of Japan) were activated as standards. After a suitable time, the gamma-ray spectra of activated samples were counted using the Ge detector at the College of Science and Engineering, Aoyama Gakuin University, Japan. Details of the analytical procedures are described in Fukuoka *et al.* (1987). Uncertainties for the trace elemental contents are listed in Table S1, as estimated from the reproducibility of standard rock JB-3 (a standard rock from the Geological Survey of Japan).

^{10}Be concentrations in the sediments were determined by accelerator mass spectrometry (AMS) using the Tandem accelerator (MALT) in the Micro Analysis Laboratory of the University of Tokyo, Japan, following the methods of Matsuzaki *et al.* (2004), Shimaoka *et al.* (2004, 2016), and Yoshida *et al.* (2011).

Dry sediment sample (~0.1 g) was dissolved in a mixture of 46% HF and 60% HNO_3 , and then about 1 mg of a Be carrier was added. After an addition of 61% HClO_4 , the solution was gently evaporated. The residue of perchlorate salts was dissolved by adding 1M HCl and 21% EDTA solution. Acetylacetone extraction into CCl_4 in the presence of EDTA is effective for eliminating many trace elements. Subsequently, Be was back-extracted into 6M HCl and the solution was dried on a hot plate. The residue was dissolved in 1M HCl and passed through a 5 mL Dowex 50W X-8 100–200-mesh cation exchange resin with 1M HCl, and Be was separated from trace amount of impurity. Beryllium hydroxide was precipitated with a

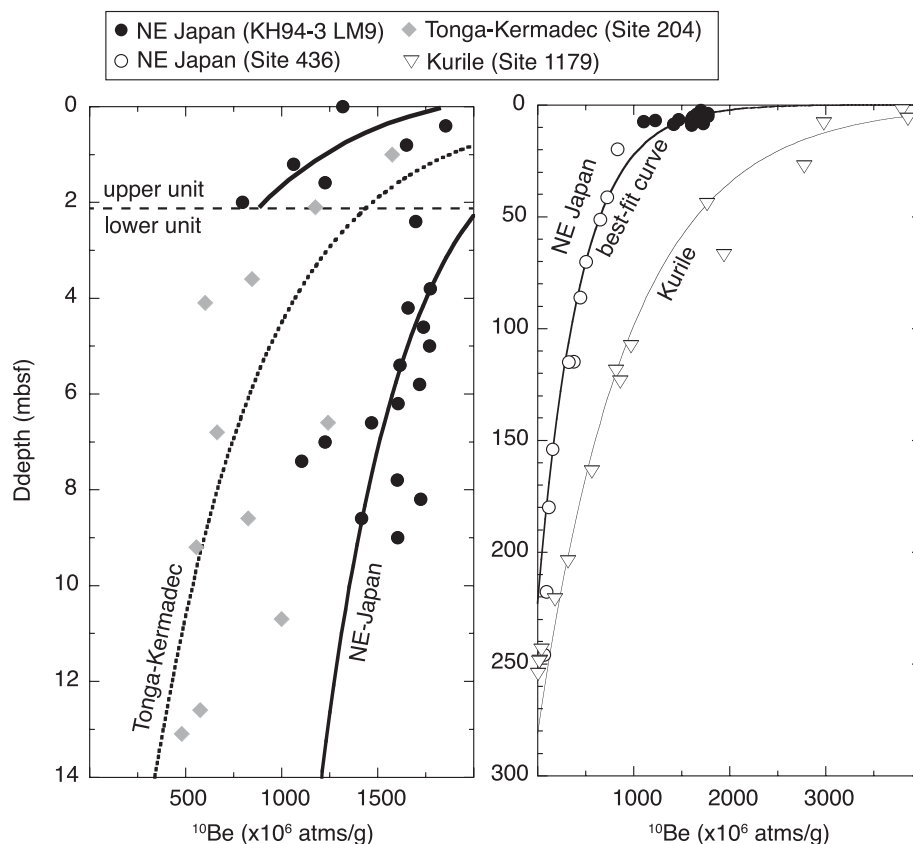


Fig. 2. Depth (mbsf) profiles of ^{10}Be in sediments (A) entering the Japan Trench at KH-94-3 LM9 and the Tonga-Kermadec Trench at DSDP Site 204, (B) entering the Japan Trench at KH-94-3 LM9 and DSDP Site 436, and Kurile Trench at ODP Site 1179. Data are from Morris *et al.* (2002b), George *et al.* (2005), Dreyer *et al.* (2010), and this study. Best-fit exponential curve (solid bold line) for the Japan Trench uses the data for KH-94-3 LM9 and Site 436. Best fit exponential curves (solid thin line and dotted line) for the Tonga-Kermadec and Kurile trenches are from the previous studies.

few drop of ammonia water (1:1). After washing with distilled water, the precipitate was re-dissolved with HCl. The Be chloride was ignited to form an oxide (BeO) in a quartz vial at 850°C . Finally, the BeO powder was collected from the vial, mixed with Nb powder (2:1), and pressed into a cathode hole with a diameter of 1 mm, which is designed to fit the ion source of the AMS. The Be extraction method is reported in Yoshida *et al.* (2011), and the sample preparation was conducted at Nihon University.

Replicate analyses of a standard sample ($^{10}\text{Be}/^9\text{Be} = 3.11 \times 10^{-11}$) indicate overall precision and accuracy of $\sim 1\%$, and blank analyses estimate that detection limit of ^{10}Be content is $1\sim 3 \times 10^5$ atoms/g (Yoshida *et al.*, 2011).

Sample preparation for ^9Be analysis involved digestion using an acid mixture of HF, HClO_4 , and HNO_3 , and final dissolution in 1 M HCl. The ^9Be in the sediment samples was analyzed using inductively coupled plasma-atomic emission spectroscopy (Shimadzu ICPS-7500) at Nihon University. Reproducibility of standard rock JB-

1a (a standard rock from the Geological Survey of Japan) indicates that overall precision and accuracy of 0.03 ppm.

RESULTS

Japan Trench sediment profile

Among 35 sediment samples in Table S2, Be isotope and INAA data of 20 samples are firstly reported in this study, but XRF and PGNA data of the samples are from Sano *et al.* (2001). All geochemical data for the other 15 sediment samples are original of this study (Table S2).

Beryllium-10 of the Japan Trench sediments (Table S2), together with Deep Sea Drilling Project (DSDP) Site 436 (Morris *et al.*, 2002b), is plotted against the depth in Fig. 2. Also, ^{10}Be in sediment columns at DSDP Site 204 (seaward of Tonga-Kermadec Trench; George *et al.*, 2005) and Ocean Drilling Program (ODP) Site 1179 (seaward of Kurile Trench; Dreyer *et al.*, 2010) are plotted against the depth for comparison (Fig. 2). The sedimentary column at KH-94-3 LM9 site is divided into upper and

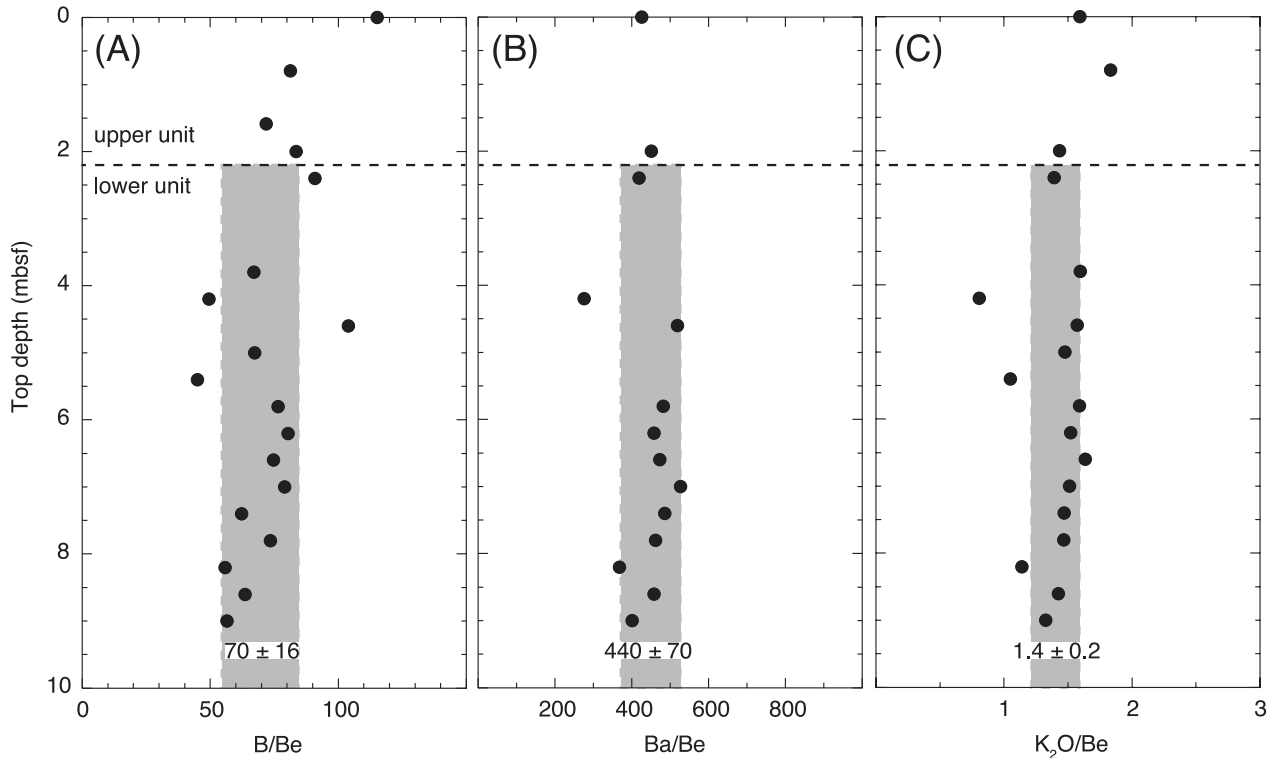


Fig. 3. (A) B/Be, (B) Ba/Be, and (C) K_2O/Be in sediments entering the Japan Trench at KH-94-3 LM9. B/Be, B/Zr, and K_2O/Be of the sediments in the lower layer are relatively uniform, though they are more variable in shallow sediments. Averages and standard deviations (\pm one sigma) of B/Be, B/Zr, and K_2O/Be are calculated by using data of the sediments in the lower layer (Table S2).

units by an offset at ~ 2.2 mbsf (meters beneath sea floor), reflecting the development of an accretionary prism composed of imbricate thrust packets or slump deposits that are confirmed at Site 436 (Morris *et al.*, 2002b; Rabinowitz *et al.*, 2015).

At KH-94-3 LM9 site, ^{10}Be concentrations in the sediments vary from 1854 to 1105×10^6 atoms/g (Table S2), which is the same range of upper 10 m of Site 436 sediments (Morris *et al.*, 2002b). The ^{10}Be concentrations in the lower unit of KH-94-3 LM9 sediments broadly decrease with depth as expected (Fig. 2A). When we combine the KH-94-3 LM9 data with lower (>10 mbsf) portion of the Site 436 data, the total inventory of ^{10}Be in the lower unit (i.e., the total amount of ^{10}Be in the sedimentary column supplied to the subduction trench) can be calculated by integrating the best-fit curve of ^{10}Be contents versus depth in Fig. 2B. The best-fit curve is expressed as

$$y = 1604e^{-0.01376x} \quad (R^2 = 0.93), \quad (1)$$

where y is the ^{10}Be content ($\times 10^6$ atoms/g) and x is depth (m). The data are approximated by exponential curves, provided the rate of sedimentation was approximately constant during deposition of the lower unit of KH-94-3

LM9 site and Site 436 though some imbricate thrusting structures are present (Morris *et al.*, 2002b). When we ignore the ^{10}Be flux of the upper unit (<2.2 mbsf), the total thickness of sediment entering the trench is taken to be 220.8 m (i.e., 223.0 m minus 2.2 m). This estimation is nearly identical to that of Kurile Trench (250 m for a sedimentary column at ODP Site 1179 in Fig. 2B; Dreyer *et al.*, 2010), but distinctly thicker than that of Tonga-Kermadec Trench (25 m a sedimentary column at DSDP Site 204 in Fig. 2B; George *et al.*, 2005).

Assuming a density of 1680 kg/m^3 of the sediment (Shipboard Scientific Party, 1980; Site 436 in Figs. 1A and 2B), integration of Eq. (1) from 2.2 m to 223.0 m yields a total ^{10}Be inventory of 1.81×10^{14} atoms in a column of the Japan Trench ($1 \text{ m} \times 1 \text{ m} \times 220.8 \text{ m}$). The calculation method is the same as the previous studies (George *et al.*, 2005; Dreyer *et al.*, 2010). The average ^{10}Be content in the Japan Trench is calculated to be 488×10^6 atoms/g, and this value is comparable with that of the Kurile Arc (574×10^6 atoms/g; Dreyer *et al.*, 2010). Using the ^{10}Be inventory and the average Be content in the lower unit sediments (1.55 ppm), the $^{10}Be/{}^9Be$ flux of the sedimentary column entering the trench is calculated to be 471×10^{-11} . This value is also comparable with that in the Kurile Arc (577×10^{-11} ; Dreyer *et al.*, 2010), but

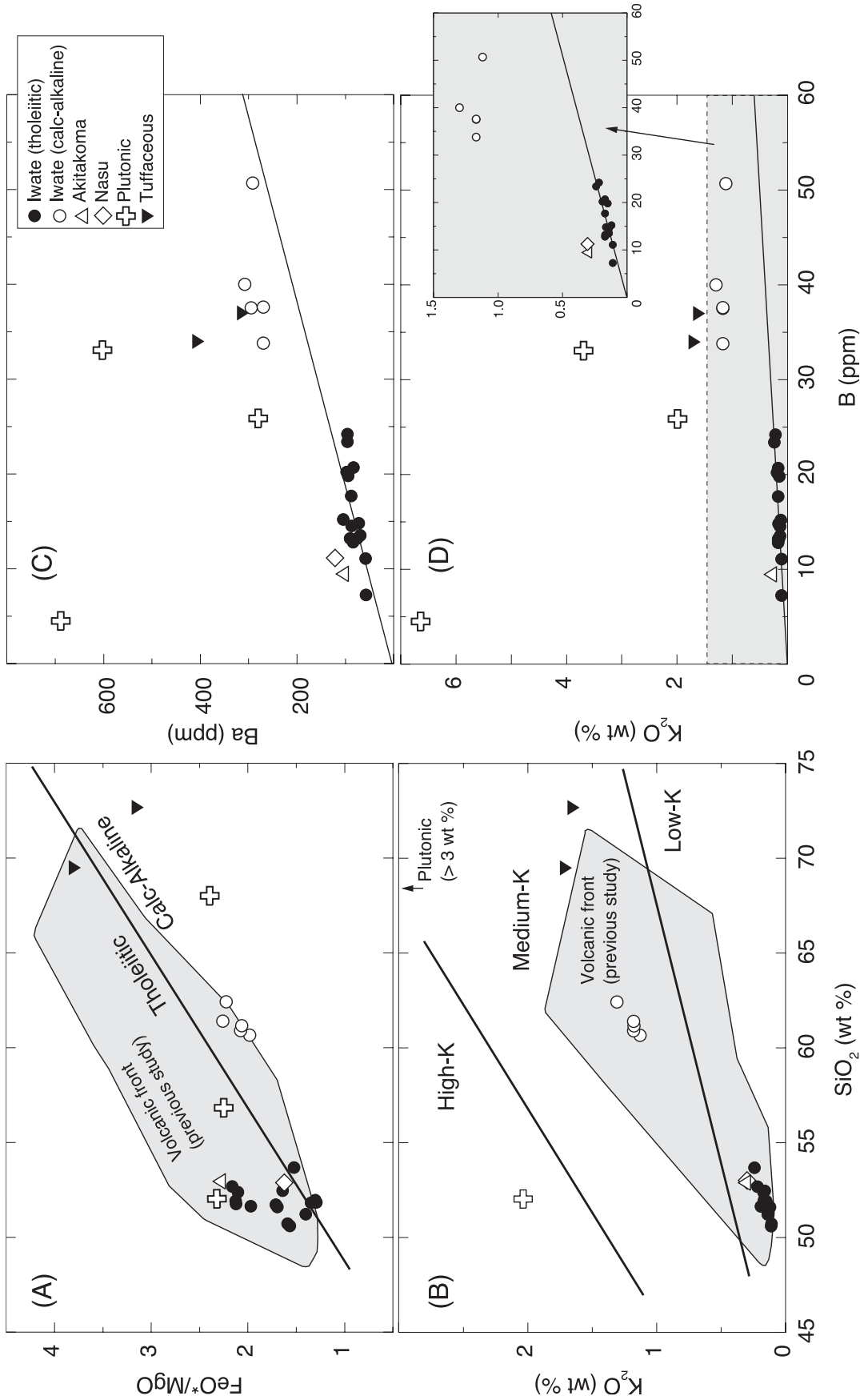


Fig. 4. Plots of (A) FeO*/MgO and (B) K₂O versus SiO₂, and (C) Ba and (D) K₂O versus B for the Iwate, Akitakoma, and Nasu lavas. Also shown are the compositions of plutonic and tuffaceous rocks that constitute the basement of the Iwate volcano. Values are normalized to 100 wt. % totals. The fields for tholeiitic and calc-alkaline rocks in the FeO*/MgO versus SiO₂ diagram are from Miyashiro (1974). The subdivision of rocks in the SiO₂ versus K₂O diagram is from Gill (1981). Two standard deviations of repeated sample analyses are generally less than the sizes of the symbols (Table S1). Published data are from Kimura and Yoshida (2006). FeO*: Fe totals are reported as FeO wt%.

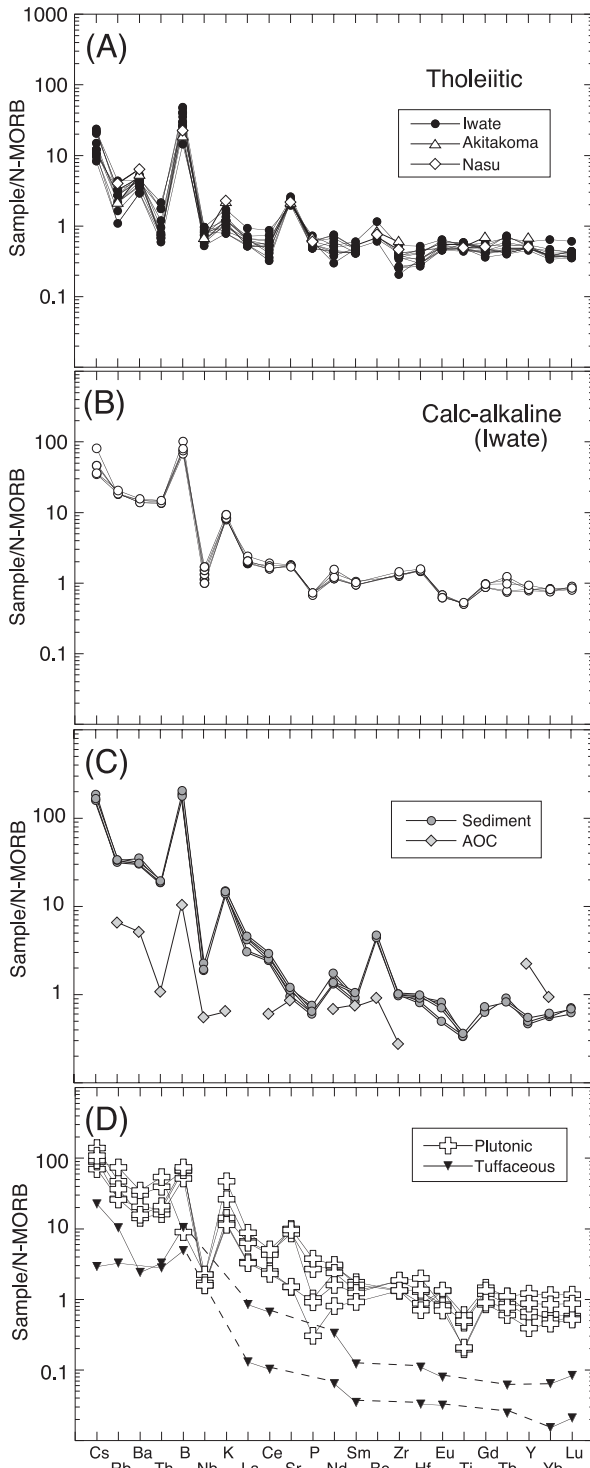


Fig. 5. N-MORB (Gale *et al.*, 2013) normalized incompatible trace element diagrams for (A) tholeiitic lavas in NE Japan, (B) calc-alkaline lavas from Iwate volcano, (C) AOC and sediments from the lower unit of the Japan Trench, and (D) plutonic and tuffaceous rocks that constitute the basement of the Iwate volcano. Data for the AOC are from McCulloch and Gamble (1991), Smith *et al.* (1995), Tatsumi and Kogiso (1997), and Kelley *et al.* (2002).

higher than values in the Tonga-Kermadec Arc (198×10^{-11} ; George *et al.*, 2005).

Figure 3 shows that B/Be, B/Zr, and K_2O/Be are relatively uniform in the deeper levels of the lower unit. We therefore consider that the B/Be, B/Zr, and K_2O/Be in the Japan Trench sediments are constant until deep levels (>100 m; Sano *et al.*, 2001); compositions of the descending sediments are compared with those of NE Japan arc lavas by using the B/Be, B/Zr, and K_2O/Be in the discussion.

NE Japan arc lavas

Among 27 rocks samples listed in Table S1, XRF and PGNA data of 9 samples are from Sano *et al.* (2001), and all Be data are from Shimaoka *et al.* (2016), but all other data are firstly reported in this study. The Iwate lavas are classified into two types: low alkali tholeiitic and calc-alkaline series (Figs. 4A and B). In contrast, both the Akitakoma and Nasu lavas belong to the tholeiitic series. Crustal contamination has major effects on the compositions of arc magmas, and these effects can be identified by plotting the contents of B against Ba and K_2O (Figs. 4C and D). All tholeiitic lavas from the Iwate volcano fall on a single linear array, suggesting little or no effect from the assimilation of crustal rocks (plutonic and tuffaceous) that have high K_2O/B and Ba/K ratios. On the other hand, Akitakoma, Nasu, and Iwate calc-alkaline lavas fall considerably above the line of the Iwate tholeiitic lavas, and this might show the effects of crustal contamination. Since the present geochemical data are not suited to estimate the effects of crustal contamination quantitatively, we selected the samples least likely affected by crustal contamination (i.e., the Iwate tholeiitic lavas) to estimate ratio of sediment recycling in the NE Japan Arc.

Trace element characteristics of lavas are simply illustrated by normalizing their trace element contents to that of normal MORB (Fig. 5). The N-MORB normalized trace element patterns for lavas from the Iwate tholeiitic lavas show enrichments in Ba, B and Be (Figs. 5A and B), which is a feature common to arc magmas (Morris *et al.*, 1990; Ryan *et al.*, 1995). On the other hand, the enrichments in Ba, B and Be are not obvious for crustal rocks (Fig. 5D), suggesting that main mechanism of the enrichments is not crustal contamination as we already have shown in Figs. 4C and D. The enrichment is probably caused by metasomatism of the mantle source rocks by slab-derived fluids as we discussed below.

The ^{10}Be contents in the Iwate tholeiitic lavas are 0.11 – 0.75×10^6 atoms/g (Table S1) with an average value of 0.213×10^6 atoms/g, which is near the lower end of the entire range of other arc lavas (Tera *et al.*, 1986; Morris *et al.*, 1990; George *et al.*, 2003, 2005; Dreyer *et al.*, 2010). The ^{10}Be contents are roughly positively corre-

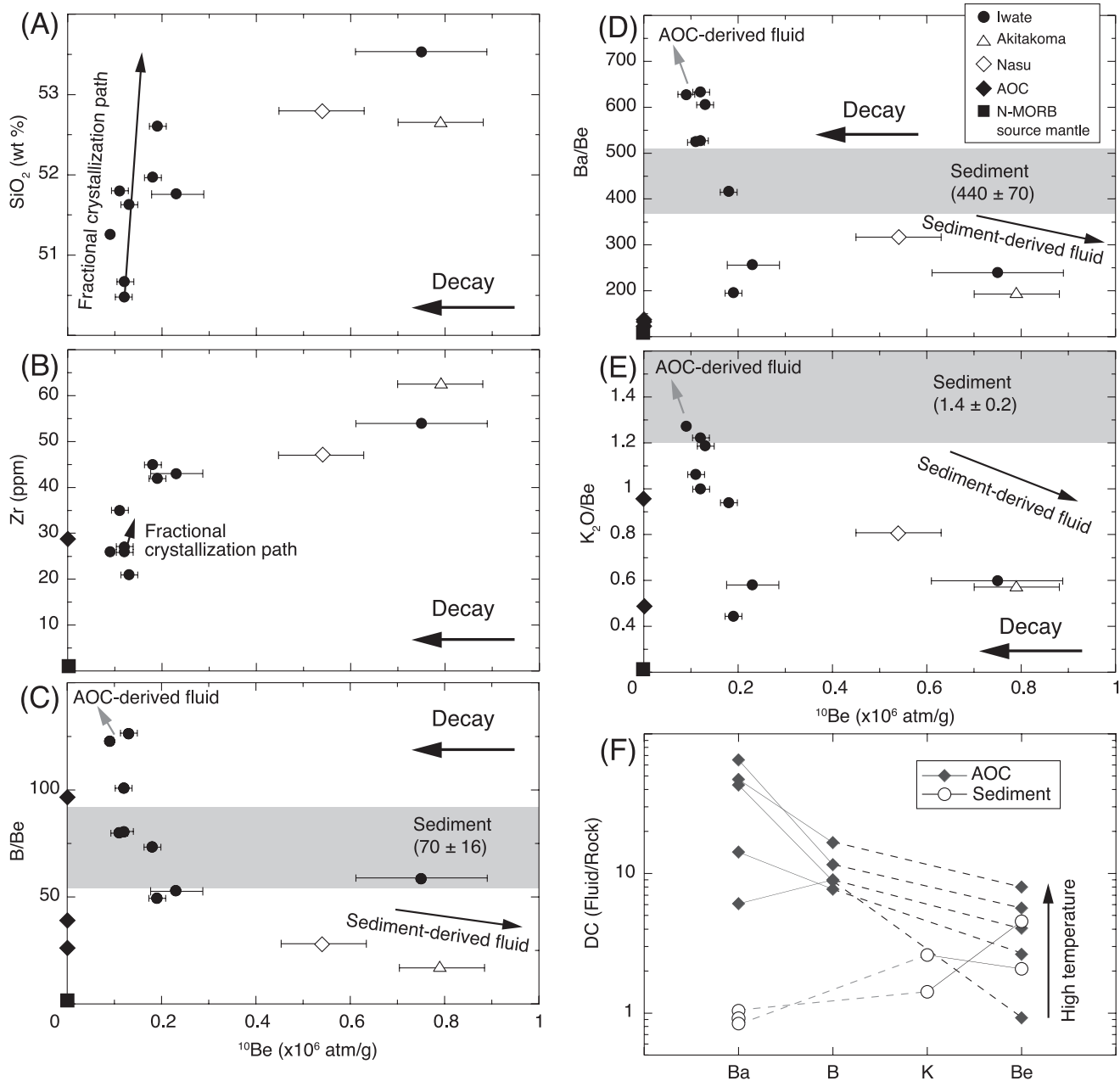


Fig. 6. (A–E) Plots of (A) SiO_2 , (B) Zr, (C) B/Be, (D) Ba/Be, and (E) $\text{K}_2\text{O}/\text{Be}$ versus ^{10}Be for the Iwate, Akitakoma, and Nasu lavas. Also shown in (A) and (B) is a fractional crystallization path calculated by a least-squares mixing calculation for Iwate tholeiite lavas (Sano *et al.*, 2001). N-MORB mantle composition is from Salters and Stracke (2004), and AOC compositions are from data of ODP Site 1179 (Sano and Hayasaka, 2004; Dreyer *et al.*, 2010). B/Be, Ba/Be, and $\text{K}_2\text{O}/\text{Be}$ of the sediments are from Fig. 3. (F) Distribution coefficient between fluid and rock (DC_{FR}) under high pressure and temperature conditions for sediments (Johnson and Plank, 1999; Martindale *et al.*, 2013) and AOC (Kessel *et al.*, 2005). Arrows with “Decay” in (A)–(D) are the directions that ^{10}Be content decreases with time. Error bars show the two standard deviations estimated by quadratic propagation of statistical errors in each calculation stage (Table S1; Shimaoka *et al.*, 2016).

lated with SiO_2 and several incompatible trace elements such as Zr (Figs. 6A and B). This correlation is difficult to interpret by simple fractional crystallization process. A least-squares mixing calculation for Iwate tholeiite

lavas, using major element chemistry, indicates that the most differentiated lava is produced by subtraction of 15% of phenocryst phases (olivine, plagioclase and augite) from the most primitive magma (Sano *et al.*, 2001). How-

ever, examination of ^{10}Be and incompatible trace element concentrations by using Rayleigh fractional crystallization equation shows that the large variation of ^{10}Be concentrations ($0.11\text{--}0.75 \times 10^6$ atm/g) are not explained by the 15% fractional crystallization (see fractional crystallization paths in Figs. 6A and B).

The positive correlation between the ^{10}Be and SiO_2 cannot be explained by crustal contamination because crustal components with high SiO_2 are free of ^{10}Be . The large variation of ^{10}Be concentrations would reflect heterogeneity of slab-derived fluids (see Section “Discussion”).

DISCUSSION

^{10}Be -B-Ba-K-Be systematics and the significance of slab-derived fluid

As explained above, a large variation of ^{10}Be concentrations in the Iwate tholeiite lavas is difficult to interpret by the simple fractional crystallization process (Figs. 6A and B). Since crustal contaminations for the Iwate tholeiite lavas are negligibly small (Figs. 4 and 5), the other possible components to produce the large compositional variations are slab-derived fluids. Among slab-derived fluids, generation of the NE Japan Arc magmas is believed to include contributions from both subducted sediments and AOC (Sano *et al.*, 2001; Hanyu *et al.*, 2006; Kimura and Yoshida, 2006; Nakamura and Iwamori, 2009). This suggestion is based on distinct B-, Ba-, and Be-enrichments of the subducted sediments and AOC (Fig. 5C). A primary factor controlling the production of the arc magma is hydrous fluid, which is most likely derived from dehydration reactions within the sediments and AOC of the subducting plate (Tatsumi, 1989).

In order to identify involvement of the slab-derived fluids components in mantle wedge, the B-Ba-K-Be systematics are used (Figs. 6C, D, and E) because these four elements have similar solid/melt bulk distribution coefficients (DC_{SM}) during the melting of peridotites and during shallow-level crystallization of basaltic magma (Chaussidon and Libourel, 1993; Leeman *et al.*, 1994; Leeman and Sisson, 1996). Examination of the melting in the mantle wedge and fractional crystallization in the magma chamber has shown that ratios of these elements in the Iwate tholeiite lavas are not changed beyond analytical errors (Sano *et al.*, 2001). We therefore suggest that these ratios in the NE Japan basalts are representative of their source mantle.

In Fig. 6, MORB-source mantle is assumed to be a mantle end-member in the mantle wedge, because the wedge under the NE Japan Arc was similar to MORB-source mantle prior to the addition of slab-derived fluids (Hanyu *et al.*, 2006; Kimura and Yoshida, 2006;

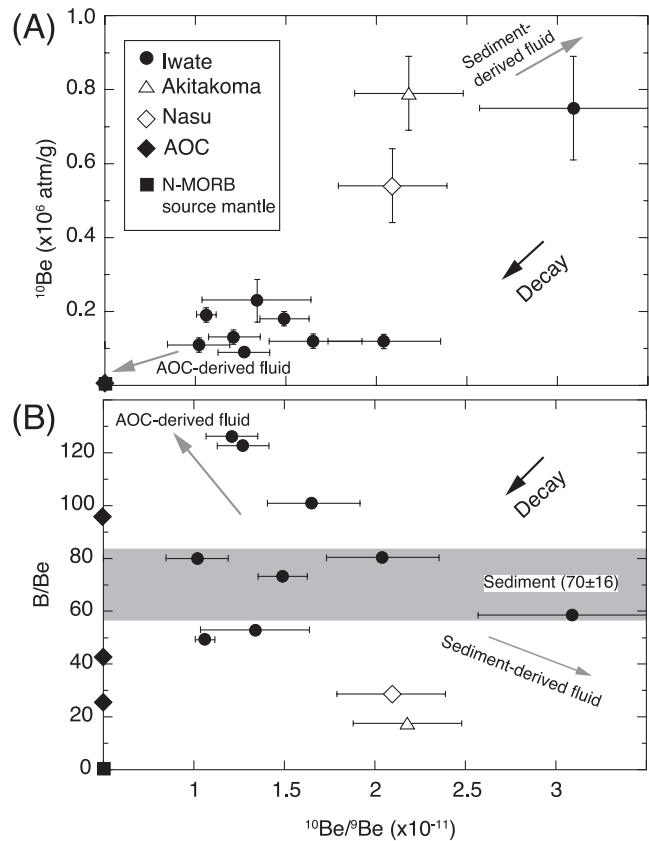


Fig. 7. Plots of (A) ^{10}Be and (B) B/Be versus $^{10}\text{Be}/^9\text{Be}$ for the Iwate, Akitakoma, and Nasu lavas, together with N-MORB source mantle and AOC. Data sources are the same as Fig. 6.

Nakamura and Iwamori, 2009; Miyazaki *et al.*, 2015). Averaged B/Be , Ba/Be and $\text{K}_2\text{O}/\text{Be}$ in the lower unit of the Japan Trench sediments are adopted for the original ratios of the sediments (Fig. 3). These ratios are similar to those of Plank and Langmuir (1998), an average for the entire sedimentary column entering the Japan Trench.

The B/Be , Ba/Be and $\text{K}_2\text{O}/\text{Be}$ are negatively correlated with ^{10}Be , and these correlations are gently concave upward. These correlations are probably explained by mixing among three components, the mantle wedge, AOC-derived fluid and sediment-derived fluid. Similar negative correlations are also confirmed in $^{10}\text{Be}/^9\text{Be}$ versus B/Be diagram (Fig. 7B).

Figure 7A shows that $^{10}\text{Be}/^9\text{Be}$ values are positively correlated with ^{10}Be , and this correlation is explained by an addition of the sediment-derived fluid to the MORB-source mantle and/or AOC-derived fluid whose compositions are near the origin. A mixing end member with low B/Be , Ba/Be , $\text{K}_2\text{O}/\text{Be}$ in Figs. 6 and 7 is certainly sediment-derived fluid. This suggestion is consistent with experimental data of distribution coefficient between fluid and rock (DC_{FR}) in Fig. 6F. Since DC_{FR} of Ba is lower

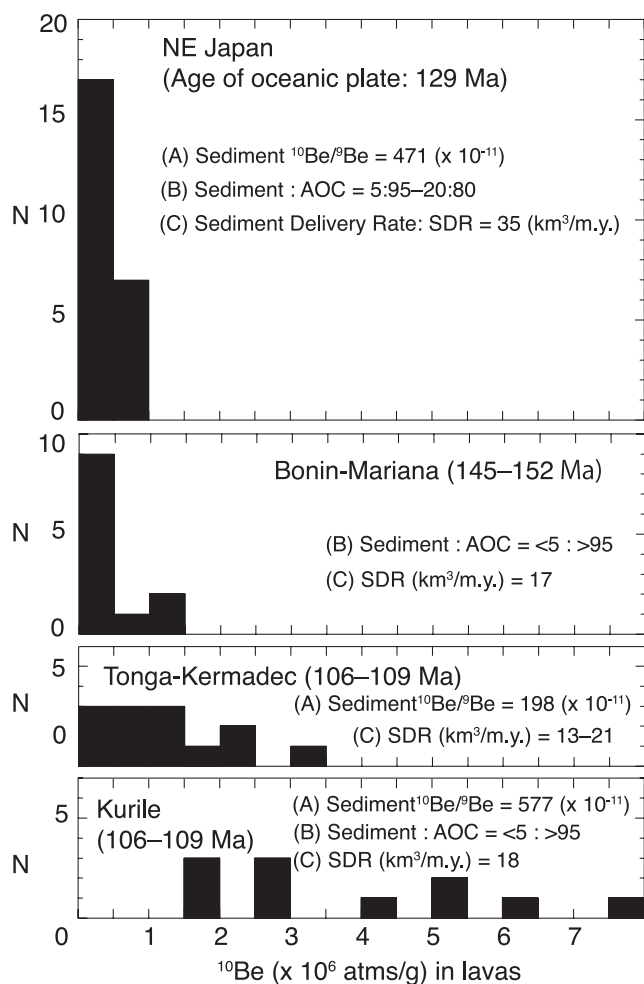


Fig. 8. Histogram showing ^{10}Be contents in active volcanoes from four cold arcs (NE Japan, Bonin-Mariana, Tonga-Kermadec, and Kurile arcs). ^{10}Be data are from Tera *et al.* (1986), Morris *et al.* (1990), George *et al.* (2005), and Shimaoka *et al.* (2016). Also shown in the diagrams are ages of subducting Pacific plate at the four cold arcs (Syracuse *et al.*, 2010), and three parameters for sediment input from the trench; (A) $^{10}\text{Be}/^9\text{Be}$ of descending sediments (George *et al.*, 2005; Dreyer *et al.*, 2010; this study), (B) ratio of sediment- to AOC-derived fluids (Ishikawa and Tera, 1997, 1999; Sano *et al.*, 2001), and (C) Sediment Delivery Rate, SDR (Clift and Vannucchi, 2004).

than that of Be during sediment dehydration process (Johnson and Plank, 1999; Martindale *et al.*, 2013), the sediment-derived fluid has lower Ba/Be than descending sediments (Figs. 3 and 6D). On the other hand, DC_{FRS} of Ba and B are higher than that of Be during the AOC dehydration process (Kessel *et al.*, 2005). We therefore suggest that a mixing end member with high B/Be, Ba/Be, $\text{K}_2\text{O}/\text{Be}$ in Figs. 6 and 7 is the AOC-derived fluid, though B/Be, Ba/Be, $\text{K}_2\text{O}/\text{Be}$ of the AOC is lower than the mixing end member.

Another candidate of the mixing end member with high B/Be, Ba/Be and $\text{K}_2\text{O}/\text{Be}$ in Figs. 6 and 7 is hydrous fluid derived from serpentinized peridotites, but the AOC is a better candidate, because Ba and K_2O contents of the AOC (Sano and Hayasaka, 2004; Dreyer *et al.*, 2010) is distinctly higher than those of the serpentinized peridotites (Savov *et al.*, 2005, 2007).

One emphatic point in Fig. 7B is that B/Be is not positively correlated with $^{10}\text{Be}/^9\text{Be}$ that was confirmed at relatively hot subduction zones (Aleutian, Central America, Andes and Bismarck arcs: Morris *et al.*, 1990). Ryan and Chauvel (2014) proposed that this correlation is produced by two end components mixing between serpentinite-derived fluid and mantle wedge. In this model, the serpentinite-derived fluid is assumed to be the end component with high B/Be and $^{10}\text{Be}/^9\text{Be}$, and mantle wedge is proposed to be MORB-source mantle whose compositions plot near the origin. However, the B/Be is negatively correlated with $^{10}\text{Be}/^9\text{Be}$ in the cold NE Japan Arc (Fig. 7B), suggesting that the model of Ryan and Chauvel (2014) inapplicable to the NE Japan Arc. We would not reject the involvement of the serpentinite-derived fluid in the source mantle of NE Japan arc, however our data have no positive evidence.

We also consider decay of ^{10}Be for one possible mechanism to explain the negative correlations in Figs. 6C, D, E, and 7B that are concave upwards. ^{10}Be concentrations would decrease (directions of arrows in Figs. 6C, D, E, and 7B) by the decay when recycling time of the sediments are long.

Ratios of sediment recycling at cold subduction zones

In order to evaluate the sediment recycling, ^{10}Be contents in the Iwate tholeiite lavas are compared with those in lavas from other arcs (Bonin-Mariana, Tonga-Kermadec, and Kurile) in Fig. 8. To simplify our discussion, we have selected only data of arcs with cold subduction zones (age of descending slab is older than 100 Ma; Syracuse *et al.*, 2010). Figure 8 shows that ^{10}Be of NE Japan and Bonin-Mariana arcs are lower than those of Tonga-Kermadec and Kurile arcs. Similar to conclusion of previous report (Morris *et al.*, 2002a), ratios of subducted ^{10}Be recycled in NE Japan Arc is the lowest among all subduction zones on the Earth.

We explain the low level of ^{10}Be observed in the NE Japan by (1) low level of ^{10}Be in subducted sediment, (2) a low extraction rate of Be from subducted slab, (3) a long travel time of sediment recycling, and/or (4) shallow crustal contamination.

Data compiled in Fig. 8 indicate that the factor (1) is not likely, because subducted sediments at Japan Trench do not show a low level of ^{10}Be compared to other trenches. Our data for Japan Trench sediments indicate that sediment input at the trench is within the ranges char-

acterized by other cold subduction zone settings; $^{10}\text{Be}/^{9}\text{Be}$ of NE Japan Trench is between those of Tonga-Kermadec and Kurile trenches (Fig. 8). Figure 8 also shows that the source of NE Japan Arc lavas has higher sediment/AOC ratios (Sano *et al.*, 2001; Hanyu *et al.*, 2006; Kimura and Yoshida, 2006; Nakamura and Iwamori, 2009) than those of Bonin-Mariana and Kurile arcs (Ishikawa and Tera, 1997, 1999). Moreover, sediment delivery rate (SDR) beneath the NE Japan Arc is higher than those of the other cold subduction zones (Fig. 8; Clift and Vannucchi, 2004).

It is necessary to consider tectonic accretion and/or erosion during subduction when estimating the subducting fraction of the total sedimentary column. If subduction zones provide suitable conditions for the formation of an accretionary prism, the uppermost ^{10}Be -rich sediments largely escape from subduction. However, the Japan Trench is at present non-accretionary in nature (von Huene and Scholl, 1991; Clift and Vannucchi, 2004), meaning that most of the sedimentary column is being subducted. Instead, we propose deeper sediment underplating or erosion as the plate subducts beneath the NE Japan Arc (von Huene and Scholl, 1991). A seminal review of the descending slab reported that 80% of the Japan Trench sediments are subducted, and even in accretionary active margins ~70% of the sedimentary column is likely to be subducted to great depths below the fore arc (von Huene and Scholl, 1991). However, recent studies on off-Miyagi region of the NE Japan Arc have highlighted complicated sediment subduction at the Japan Trench (Kodaira *et al.*, 2012; Chester *et al.*, 2013) and relatively old ages of sediment below the decollement (Rabinowitz *et al.*, 2015). Deformation structures formed by slumping and multi-faults are present at Integrated Ocean Drilling Program (IODP) Site C00019 (Fig. 1A). The complicated sediment structure as well as imbricate thrusting would reduce the ^{10}Be amount subducted to depth (Morris *et al.*, 2002b; Morris and Ryan, 2004).

Next, we examine factor (2), because concentrations of slab-derived elements in arc magmas partly depend on the element flux via sediment subduction, not simply on the sediment composition (Plank and Langmuir, 1993, 1998). Factor (2) presents a possible explanation because DC_{FR} of Be during dehydration increases with increasing temperature at high pressure conditions (Fig. 6F; Johnson and Plank, 1999; Kessel *et al.*, 2005; Martindale *et al.*, 2013). Because the subducting slab is old and cold at NE Japan Arc, the low ratio of the sediment recycling would be reduced by the low DC_{FR} of Be at low temperature conditions.

Factor (3) is one possible answer, because hydrous minerals in the sediments are probably subducted and liberate the sediment-derived fluid at deep levels (>180 km; Fig. 1B). A long travel time is required to explain the

deep subduction and recycling of the sediments. The convergence rate (10 cm/year) and subduction angle (30°) of the descending Pacific slab (Hasegawa *et al.*, 1994; Clift and Vannucchi, 2004) estimate that the recycling time is 4.9 Myr when the sediment is subducted to 180 km and the sediment-derived fluids ascend to a depth of magma generation beneath the volcanic front (e.g., 50 km; Tatsumi *et al.*, 1983; Kimura and Yoshida, 2006). Here we do not consider the migration time after magma generation because excess ^{226}Ra in the arc lavas indicates magma extraction and ascent on timescales of less than ~3000 years (Spiegelman and Elliott, 1993).

An alternative explanation of the long recycling time in the NE Japan Arc is that additional time has elapsed since the subduction and dehydration of the sediments, which is not accounted for in a simple transport model. The long transport time may reflect complex transport processes. Tatsumi (1989) for example proposes that the migration of fluids from the subducted slab to the magma source involves the following two-step process. (1) A hydrous peridotite layer is formed by the addition of slab-derived fluids beneath the forearc region, and this layer would be dragged downwards on the slab by the subduction of the Pacific Plate. (2) Hydrous minerals in the hydrous peridotite layer decompose to release fluids beneath the volcanic front, resulting in the formation of hydrous columns. When the migration front of the hydrous column reaches the region of the solidus temperature, partial melting occurs to produce the primary magma.

The processes of partial melting and magmatic evolution are also complex. Recent studies of NE Japan Arc lavas proposes that tholeiitic magmas are produced via anatexis of amphibolitic crust by underplating and/or intrusion of mantle-derived calc-alkaline basalt magmas into the NE Japan crust (Tatsumi *et al.*, 2008; Takahashi *et al.*, 2013). In this case, the long travel time of sediment recycling is caused by a long period of solidification of the mantle-derived calc-alkaline basalt magma beneath and/or within the crust. In any case, the introduction of complex transport processes to sediment recycling favors the long travel times to explain the low ratio of subducted ^{10}Be recycled in NE Japan Arc.

Factor (4) provides the explanation that crustal contamination could result in dilution of the young magmas, and therefore lowering of the ^{10}Be . However, the positive correlation between ^{10}Be and SiO_2 in Fig. 6A is opposite to the expected effect of crustal contamination. Furthermore, the selection of only Iwate tholeiitic lavas (with the least likely affected by crustal contamination) in the discussion essentially rules out any possible contribution from factor (4).

Finally, we discuss the possible effect of contamination from young marine sedimentary rocks to Kurile volcanoes that have relatively high ^{10}Be contents (Fig. 8).

This process has recently been proposed at Esan volcano in Hokkaido area between the NE Japan and Kurile arcs (Fig. 1A). Shimaoka *et al.* (2016) found that Esan lavas have significantly higher ^{10}Be contents (up to 2.13×10^6 atms/g) and $^{10}\text{Be}/^9\text{Be}$ (up to 91×10^{-12}) than other Japanese volcanoes. Since young marine sedimentary rocks of late Quaternary age are present near the surface in the area around Esan volcano (Ando, 1974), one plausible mechanism to generate the high ^{10}Be contents is contamination of the young sediments (Shimaoka *et al.*, 2016). Some rocks with high ^{10}Be contents in the Kurile lavas might have been contaminated by the young sediments, although information on the geology and petrology of the Kurile volcanoes necessary to establish a dehydration model is unavailable.

CONCLUSIONS

The sedimentary column at the Japan Trench is divided into upper and lower units by an offset at ~ 2.2 mbsf. An integration of the ^{10}Be -depth profile in the lower unit and previously reported values yields an average ^{10}Be content in the Japan Trench of 488×10^6 atms/g, and this estimation is similar to values reported for the Kurile Arc. Since B/Be, Ba/Be, $\text{K}_2\text{O}/\text{Be}$ of the lower unit are probably constant until deep levels (>100 m), these ratios are used to examine sediment recycling at the NE Japan Arc.

The trace element characteristics of Akitakoma, Nasu, and Iwate calc-alkaline lavas may be affected by contamination of crustal rocks, but tholeiitic lavas from Iwate volcano have no or little contribution from crustal contamination.

^{10}Be -B-Ba-K-Be systematics of Iwate tholeiite lavas cannot be explained by simple fractional crystallization process and their varieties are produced by three component mixing among sediment-derived fluid, AOC derived fluid, and MORB-source mantle. Geochemical data from the NE Japan Arc provide no evidence for the involvement of serpentine-derived fluid in the magma sources.

^{10}Be contents in the Iwate tholeiite lavas are near the lowest end among cold subduction zones (Bonin-Mariana, Tonga-Kermadec, and Kurile arcs). Comparisons between ^{10}Be inputs from trenches and ^{10}Be outputs from arc volcanoes show that ^{10}Be recycling at the NE Japan Arc is distinctly lower than other cold arcs. The low ratio of ^{10}Be recycling is explained by three factors; (1) significant reduction of ^{10}Be from descending sediments, (2) a low extraction rate of Be from the subducted slab, and/or (3) a long travel time during sediment recycling. Factors (2) and (3) arise from the low temperature of the descending slab beneath the NE Japan Arc.

Acknowledgments—The PGNA has been carried out at the Inter-University Laboratory for the Joint use of Japan Atomic Energy Research Institute facilities. We thank Yoshihiro

Yamazaki, Yuko Saito, Mitsunori Ishimoto, and Hiroyuki Sawahata for analytical support. Reviews by two anonymous reviewers, editorial comments by Hikaru Iwamori, and English editing by Chris Conway were appreciated. This research was supported financially by the Ishibashi Memorial Foundation at Risso University and the National Museum of Nature and Science.

REFERENCES

- Ando, S. (1974) Geology and petrology of Esan volcano, Hokkaido Japan. *J. Mineral. Petrol. Econom. Geol.* **69**, 302–312 (in Japanese).
- Bebout, G. E. (2007) Metamorphic chemical geodynamics of subduction zones. *Earth Planet. Sci. Lett.* **260**, 373–393.
- Benton, L. D., Ryan, J. G. and Tera, F. (2001) Boron isotope systematics of slab fluids as inferred from a serpentine seamounts, Mariana forearc. *Earth Planet. Sci. Lett.* **187**, 273–282.
- Chaussidon, M. and Libourel, G. (1993) Boron partitioning in the upper mantle: an experimental and ion probe study. *Geochim. Cosmochim. Acta* **57**, 5053–5062.
- Chester, F. M., Rowe, C., Ujiie, K., Kirkpatrick, J., Regalla, C., Remitti, F., Moore, C. J., Toy, V., Wolfson-Schwehr, M., Bose, S., Kameda, J., Mori, J. J., Brodsky, E. E., Eguchi, N., Toczko, S. and Expedition 343 and 343T Scientists (2013) Structure and composition of the plate-boundary slip zone for the 2011 Tohoku-Oki earthquake. *Science* **342**, 1208–1210.
- Clift, P. and Vannucchi, P. (2004) Controls on tectonic accretion versus erosion in subduction zones: implications for the origin and recycling of the continental crust. *Rev. Geophys.* **42** (<http://dx.doi.org/10.1029/2003RG000127>).
- Dreyer, B. M., Morris, J. D. and Gill, J. B. (2010) Incorporation of subducted slab-derived sediment and fluid in arc magmas: B-Be- ^{10}Be - ϵNd systematics of the Kurile convergent margin, Russia. *J. Petrol.* **51**, 1761–1782.
- Elliott, T. (2003) Tracers of the slab. *Inside the Subduction Factory* (Eiler, J. and Hirschmann, M., eds.), 23–46, Geophys. Monogr. 138, American Geophysical Union.
- Elliott, T., Plank, T., Zindler, A., White, W. and Bourdon, B. (1997) Element transport from slab to volcanic front at the Mariana arc. *J. Geophys. Res.* **102**, 14,991–15,019.
- Fukuoka, T., Arai, F. and Nishio, F. (1987) Correlation of tephra layers in Antarctic ice by trace element abundances and refractive indices of glass shards. *Bull. Volcanol. Soc. Jpn.* **32**, 103–118.
- Gale, A., Dalton, C. A., Langmuir, C. L., Su, Y. and Schilling, J.-G. (2013) The mean composition of ocean ridge basalts. *Geochem. Geophys. Geosyst.* **14**, 489–518 (<http://dx.doi.org/10.1029/2012GC004334>).
- George, R., Turner, S., Hawkesworth, C., Morris, J., Nye, C., Ryan, J. and Zheng, S.-H. (2003) Melting processes and fluid and sediment transport rates along the Alaska-Aleutian arc from an integrated U-Th-Ra-Be isotope study. *J. Geophys. Res.* **108**(B5), 2252 (<http://dx.doi.org/10.1029/2002JB001916>).
- George, R., Turner, S., Morris, J., Plank, T., Hawkesworth, C. and Ryan, J. (2005) Pressure-temperature-time paths of sedi-

- ment recycling beneath the Tonga-Kermadec arc. *Earth Planet. Sci. Lett.* **233**, 195–211.
- Gill, J. (1981) *Orogenic Andesites and Plate Tectonics*. Springer-Verlag, 390 pp.
- Hanyu, T., Tatsumi, Y., Nakai, S.-I., Chang, Q., Miyazaki, T., Sato, K., Tani, K., Shibata, T. and Yoshida, T. (2006) Contribution of slab melting and slab dehydration to magmatism in the NE Japan arc for the last 25 Myr: Constraints from geochemistry. *Geochem. Geophys. Geosyst.* **8**, Q08002 (<http://dx.doi.org/10.1029/2005GC001220>).
- Hasegawa, A., Horiuchi, S. and Umino, N. (1994) Seismic structure of the northeastern Japan convergent margin: a synthesis. *J. Geophys. Res.* **99**, 22295–22311.
- Imai, N., Terashima, S., Itoh, S. and Ando, A. (1995) 1994 compilation of analytical data for minor and trace elements in seventeen GSJ geochemical reference samples, “igneous rock series”. *Geostand. Newslett.* **19**, 135–213.
- Ishikawa, T. and Nakamura, E. (1994) Origin of the slab component in arc lavas from across-arc variation of B and Pb isotopes. *Nature* **370**, 205–208.
- Ishikawa, T. and Tera, F. (1997) Source, composition and distribution of the fluid in the Kurile mantle wedge: Constraints from across-arc variations of B/Nb and B isotopes. *Earth Planet. Sci. Lett.* **152**, 123–138.
- Ishikawa, T. and Tera, F. (1999) Two isotopically distinct fluid components involved in the Mariana arc: Evidence from Nb/B ratios and B, Sr, Nd, and Pn isotope systematics. *Geology* **27**, 83–86.
- Iwamori, H. (2007) Transport of H₂O beneath the Japan arc and its implications for global water circulation, *Chem. Geol.* **239**, 182–198.
- Iwamori, H. and Albarède, F. (2008) Decoupled isotopic record of ridge and subduction zone processes in oceanic basalts by independent component. *Geochem. Geophys. Geosyst.* **9**, Q04033 (<http://dx.doi.org/10.1029/2007GC001753>).
- Johnson, M. C. and Plank, T. (1999) Dehydration and melting experiments constrain the fate of subducted sediments. *Geochem. Geophys. Geosyst.* **1**, 1999GC000014.
- Kawamoto, T., Kanzaki, M., Mibe, K., Matsukage, K. N. and Ono, S. (2012) Separation of supercritical slab-fluids to form aqueous fluid and melt components in subduction zone magmatism. *Proc. Natl. Acad. Sci. USA* **109**, 18695–18700.
- Kelley, K. A., Plank, T., Ludden, J. and Staudigel, H. (2002) Compositions of altered oceanic crust at ODP Sites 801 and 1149. *Geochem. Geophys. Geosyst.* **4**, 8910 (<http://dx.doi.org/10.1029/2002GC000435>).
- Kessel, R., Schmidt, M. W. and Pettke, T. (2005) Trace element signature of subduction-zone fluids, melts and supercritical fluids at 120–180 km depth. *Nature* **437**, 724–727.
- Kimura, J.-I. and Yoshida, T. (2006) Contributions of slab fluids, mantle wedge and crust to the origin of Quaternary lavas in the NE Japan Arc. *J. Petrol.* **47**, 2185–2232.
- Kimura, J.-I., Gill, J. B., Skora, S., van Keken, P. E. and Kawabata, H. (2016) Origin of geochemical mantle components: Role of subduction filter. *Geochem. Geophys. Geosyst.* **17**, doi:10.1002/2016GC006343.
- Kodaira, S., No, T., Nakamura, Y., Fujiwara, T., Kaiho, Y., Miura, S., Takahashi, N., Kaneda, Y. and Taira, A. (2012) Coseismic fault rupture at the trench axis during the 2011 Tohoku-oki earthquake. *Nat. Geosci.* **5**, 646–650.
- Leeman, W. P. and Sisson, V. B. (1996) Geochemistry of boron and its implications for crustal and mantle processes. *Boron: Mineralogy, Petrology and Geochemistry* (Grew, E. S. and Anovitz, L. M., eds.), 645–707, *Rev. Mineral.* **33**, Mineralogical Society of America.
- Leeman, W. P., Carr, M. J. and Morris, J. D. (1994) Boron geochemistry of the Central American Volcanic Arc: Constraints on the genesis of subduction-related magmas. *Geochim. Cosmochim. Acta* **58**, 149–168.
- Martindale, M., Skora, S., Pickles, J., Elliott, T., Blundy, J. and Avanzinelli, R. (2013) High pressure phase relations of subducted volcanoclastic sediments from the west Pacific and their implications for the geochemistry of Mariana arc magmas. *Chem. Geol.* **342**, 94–109.
- Matsuzaki, H., Nakano, C., Yamashita, H., Maejima, Y., Miyairi, Y., Wakasa, S. and Horiuchi, K. (2004) Current status and future direction of MALT, The University of Tokyo. *Nucl. Inst. Meth. Phys. Res. B* **223–224**, 92–99.
- McCulloch, M. T. and Gamble, J. A. (1991) Geochemical and geodynamical constraints on subduction zone magmatism. *Earth Planet. Sci. Lett.* **102**, 358–374.
- Mibe, K., Kawamoto, T., Matsukage, K. N., Fei, Y. and Ono, S. (2011) Slab melting versus slab dehydration in subduction-zone magmatism. *Proc. Natl. Acad. Sci. USA* **108**, 8177–8182.
- Miyashiro, A. (1974) Volcanic rock series in island arc and active continental margins. *Am. J. Sci.* **274**, 321–355.
- Miyazaki, T., Kimura, J.-I., Senda, R., Vaglarov, B. S., Chang, Q., Takahashi, T., Hirahara, Y., Hauff, F., Hayasaka, Y., Sano, S., Shimoda, G., Ishizuka, O., Kawabata, H., Hirano, N., Machida, S., Ishii, T., Tani, K. and Yoshida, T. (2015) Missing western half of the Pacific Plate: Geochemical nature of the Izanagi-Pacific Ridge interaction with a stationary boundary between the Indian and Pacific mantles. *Geochem. Geophys. Geosyst.* **16**, 3309–3332, doi:10.1002/2015GC005911.
- Morris, J. D. and Ryan, J. G. (2004) Subduction zone processes and implications for changing composition of the upper and lower mantle. *Treatise on Geochemistry* **2.11**, 451–470.
- Morris, J. D., Leeman, W. P. and Tera, F. (1990) The subducted component in island arc lavas: constraints from Be isotopes and B-Be systematics. *Nature* **344**, 31–36.
- Morris, J. D., Gosse, J., Brachfeld, S. and Tera, F. (2002a) Cosmogenic Be-10 and the solid earth: studies in geomagnetism, subduction zone processes, and active tectonics. *Beryllium: Mineralogy, Petrology and Geochemistry* (Grew, S., ed.), 207–270, *Rev. Mineral.* **50**, Mineralogical Society of America.
- Morris, J., Valentine, R. and Harrison, T. (2002b) ¹⁰Be imaging of sediment accretion and subduction along the northeast Japan and Costa Rica convergent margins. *Geology* **30**, 59–62.
- Nakagawa, M. (1987) Geology of Iwate volcanic group, northeastern Japan. *J. Jpn. Assoc. Miner. Petrog. Econ. Geol.* **82**, 132–150 (in Japanese with English abstract).
- Nakamura, H. and Iwamori, H. (2009) Contribution of slab-

- fluid in arc magmas beneath the Japan arcs. *Gondwana Res.* **16**, 431–445.
- Nichols, G. T., Wyllie, P. J. and Stern, C. R. (1994) Subduction zone melting of pelagic sediments constrained by melting experiments. *Nature* **371**, 785–788.
- Nishiizumi, K., Imamura, M., Caffee, M. W., Southon, J. R., Finkel, R. C. and McAninch, J. (2007) Absolute calibration of ^{10}Be AMS standards. *Nucl. Instr. Meth. Phys. Res. B* **258**, 403–413.
- Notsu, K. (1983) Strontium isotope composition in volcanic rocks from the Northeast Japan Arc. *J. Volcanol. Geotherm. Res.* **18**, 531–548.
- Plank, T. (2014) The chemical composition of subducting sediments. *Treatise on Geochemistry 2nd Edition*, **4.17**, 607–629.
- Plank, T. and Langmuir, C. H. (1993) Tracing trace elements from sediment input to volcanic output at subduction zones. *Nature* **362**, 739–743.
- Plank, T. and Langmuir, C. H. (1998) The chemical composition of subducting sediment and its consequences for the crust and mantle. *Chem. Geol.* **145**, 325–394.
- Rabinowitz, H. S., Savage, H. M., Plank, T., Polissar, P. J., Kirkpatrick, J. D. and Rowe, C. D. (2015) Multiple major faults at the Japan trench: Chemostratigraphy of the plate boundary at IODP Exp. 342: JFAST. *Earth Planet. Sci. Lett.* **423**, 57–66.
- Ryan, J. G. and Chauvel, C. (2014) The subduction-zone filter and the impact of recycled materials on the evolution of the mantle. *Treatise on Geochemistry 2nd Edition*, **3.13**, 479–508.
- Ryan, J. G., Morris, J., Tera, F., Leeman, W. P. and Tsvetkov, A. (1995) Cross-arc geochemical variations in the Kurile Arc as a function of slab depth. *Science* **270**, 625–627.
- Salters, V. J. M. and Stracke, A. (2004) Composition of the depleted mantle. *Geochem. Geophys. Geosyst.* **5**, Q05004 (<http://dx.doi.org/10.1029/2003GC000597>).
- Sano, S. and Hayasaka, Y. (2004) Sr and Nd geochemistry of Hole 1179D basalts. *Proc. ODP Sci. Results* (Sager, W. W., Kanazawa, T. and Escutia, C., eds.), **191**, 1–11.
- Sano, T. (2002) Determination of major and trace element contents in igneous rocks by X-ray fluorescence spectrometer analysis. *Bull. Fuji Tokoha Univ.* **2**, 43–59 (in Japanese with English abstract).
- Sano, T., Fukuoka, T., Hasenaka, T., Yonezawa, C. and Matsue, H. (1999) Accurate and efficient determination of boron content in volcanic rocks by neutron induced prompt gamma-ray analysis. *J. Radioanal. Nucl. Chem.* **239**, 613–617.
- Sano, T., Hasenaka, T., Shimaoka, A., Yonezawa, C. and Fukuoka, T. (2001) Boron contents of Japan Trench sediments and Iwate basaltic lavas, Northeast Japan arc: estimation of sediment-derived fluid contribution in mantle wedge. *Earth Planet. Sci. Lett.* **186**, 187–198.
- Sano, T., Hasenaka, T., Sawahata, H. and Fukuoka, T. (2006) Determination of Ti, K, Su, Gd values in Geological Survey of Japan reference materials by prompt gamma neutron activation analysis. *Geostand. Geoanal. Res.* **30**, 31–37.
- Sano, T., Fukuoka, T. and Ishimoto, M. (2011) Petrological constraints on magma evolution of the Fuji volcano: a case study for the 1707 Hiei eruption. *Studies on the Origin and Biodiversity in the Sagami Sea Fossa Magna Element and the Izu-Ogasawara (Bonin) Arc* (Kuramochi, T., ed.), 471–496, Mem. Natl. Mus. Nat. Sci., Tokyo.
- Savov, I. P., Ryan, J. G., D'Antonio, M., Kelley, K. and Mattie, P. (2005) Geochemistry of serpentinized peridotites from the Mariana forearc conical seamounts, ODP Leg 125: implications for the elemental recycling at subduction zones. *Geochem. Geophys. Geosyst.* **5**, Q04J15 (<http://dx.doi.org/10.1029/2004GC000777>).
- Savov, I. P., Ryan, J. G., D'Antonio, M. and Fryer, P. (2007) Shallow slab fluid release across and along the Mariana arc-basin system: insights from geochemistry of serpentinized peridotites from the Mariana fore arc. *J. Geophys. Res.* **112**, B09205 (<http://dx.doi.org/10.1029/2006JB004749>).
- Schmidt, M. W. and Poli, S. (1998) Experimentally based water budgets for dehydrating slabs and consequences for arc magma generation. *Earth Planet. Sci. Lett.* **163**, 361–379.
- Shimaoka, A., Sakamoto, M., Hiyagon, H., Matsuzaki, H., Kaneoka, I. and Imamura, M. (2004) Meteoric ^{10}Be in volcanic materials and its behavior during acid-leaching. *Nucl. Instr. Meth. Phys. Res. B* **223–224**, 591–595.
- Shimaoka, A., Imamura, M. and Kaneoka, I. (2016) Beryllium isotopic systematics in island arc volcanic rocks from northeast Japan: Implications for the incorporation of oceanic sediments into island arc magmas. *Chem. Geol.* **443**, 158–172.
- Shipboard Scientific Party (1980) Site 436, Japan Trench outer rise, Leg 56. Initial Report of the Deep Sea Drilling Project 56, 57, 399–446, U.S. Government Printing Office.
- Smith, H. J., Spivack, A. J., Staudigel, H. and Hart, S. R. (1995) The boron isotopic composition of altered oceanic crust. *Chem. Geol.* **126**, 119–135.
- Spiegelman, M. and Elliott, T. (1993) Consequences of melt transport for uranium series disequilibrium in young lavas. *Earth Planet. Sci. Lett.* **118**, 1–20.
- Spivack, A. J., Palmer, M. R. and Edmond, J. M. (1987) The sedimentary cycle of the boron isotopes. *Geochim. Cosmochim. Acta* **51**, 1939–1949.
- Syracuse, E. M., van Keken, P. E. and Abers, G. A. (2010) The global range of subduction zone thermal models. *Phys. Earth Planet. Int.* **183**, 73–90.
- Takahashi, T., Hirahara, Y., Miyazaki, T., Senda, R., Chang, Q., Kimura, J.-I. and Tatsumi, Y. (2013) Primary magmas at the volcanic front of the NE Japan arc: coeval eruption of crustal low-K tholeiitic mantle-derived medium-K calc-alkaline basalts at Azuma volcano. *J. Petrol.* **54**, 103–148.
- Tatsumi, Y. (1989) Migration of fluid phases and genesis of basalt magmas in subduction zones. *J. Geophys. Res.* **94**, 4697–4707.
- Tatsumi, Y. and Kogiso, T. (1997) Trace element transport during dehydration processes in the subducted oceanic crust: 2. Origin of chemical and physical characteristics in arc magmatism. *Earth Planet. Sci. Lett.* **148**, 207–221.
- Tatsumi, Y., Sakuyama, M., Fukuyama, H. and Kushiro, I. (1983) Generation of arc basalt magmas and thermal structure of the mantle wedge in subduction zones. *J. Geophys. Res.* **88**, 5815–5825.
- Tatsumi, Y., Takahashi, T., Hirahara, Y., Chang, Q., Miyazaki,

- T., Kimura, J.-I., Ban, M. and Sakayori, A. (2008) New insight into andesite genesis: the role of mantle-derived calc-alkalic and crust-derived tholeiitic melts in magma differentiation beneath Zao volcano, NE Japan. *J. Petrol.* **49**, 1971–2008.
- Tera, F., Brown, L., Morris, J. and Sacks, S. (1986) Sediment incorporation in island-arc magmas: Inferences from ^{10}Be . *Geochim. Cosmochim. Acta* **50**, 535–550.
- Turner, S. and Hawkesworth, C. (1997) Constraints on flux rates and mantle dynamics beneath island arcs from Tonga-Kermadec lava geochemistry. *Nature* **389**, 568–573.
- von Huene, R. and Scholl, D. W. (1991) Observations at convergent margins concerning sediment subduction, subduction erosion, and the growth of continental crust. *Rev. Geophys.* **29**, 279–316.
- Yoshida, T., Yamagata, T., Saito, T. and Nagai, H. (2011) Distribution of ^{10}Be in deep-sea sediments from the North Pacific Ocean. *Proc. Inst. Nat. Sci., Nihon Univ.* **46**, 361–371 (in Japanese with English abstract).

SUPPLEMENTARY MATERIALS

URL (<http://www.terrapub.co.jp/journals/GJ/archives/data/51/MS468.pdf>)
Tables S1 and S2